PROBING THE INITIAL STATE WITH ISOLATED-PHOTON PRODUCTION AND DIJET INVARIANT MASS DISTRIBUTIONS IN SMALL COLLISION SYSTEMS WITH ALICE*

Sinjini Chandra

for the ALICE Collaboration

Variable Energy Cyclotron Centre, Kolkata, India
and
Homi Bhabha National Institute, Mumbai, India

Received 8 August 2022, accepted 29 August 2022, published online 14 December 2022

Isolated photons and dijets measurements in small collision systems, *i.e.*, *pp* and *pA*, probe the initial state of the collision, providing the opportunity to constrain PDFs, test pQCD predictions, and probe cold nuclear matter effects. In addition, dijet measurements are sensitive to interactions of partons with the medium produced in Pb–Pb collisions that induce modifications in jet properties. Therefore, measurements in small collision systems also offer a baseline for Pb–Pb collision measurements. In this article, we present the measurement of isolated photons and dijets in small collision systems, *pp* and *p*–Pb by ALICE. Isolated photons are measured in *pp* collisions at $\sqrt{s} = 8$ and 13 TeV and in *p*–Pb collisions at $\sqrt{s_{NN}} = 5.02$ TeV, down to $p_{\mathrm{T}} = 10$ GeV/c, extending previous measurements at these centre-of-mass energies down to small $x \sim 10^{-3}$. The dijet invariant mass is measured in *pp* and *p*–Pb collisions at $\sqrt{s_{NN}} = 5.02$ TeV within the range from 80 to 150 GeV/c^2, probing a region where medium effects are expected to be strong.

DOI:10.5506/APhysPolBSupp.16.1-A26

1. Introduction

The study of photons at large transverse momenta (p_{T}) in high-energy hadronic collisions is a valuable tool to test perturbative Quantum Chromodynamics (pQCD). Since these photons are produced directly from parton–parton hard scatterings, they can also be used to constrain the parton distribution functions (PDFs). In leading order pQCD, direct photon production

* Presented at the 29$^{\mathrm{th}}$ International Conference on Ultrarelativistic Nucleus–Nucleus Collisions: Quark Matter 2022, Kraków, Poland, 4–10 April, 2022.

can be described by two elementary processes at the parton level: quark–gluon Compton scattering and quark–antiquark annihilation. These photons from the $2 \rightarrow 2$ processes, together with the fragmentation photons generated from parton fragmentation, are usually referred to as the prompt photons. Photons from $2 \rightarrow 2$ processes provide clear constraints of the underlying parton kinematics, but making a clean separation between the different types of prompt photons is difficult. Experimentally, measuring the direct photons is complicated by the presence of large photon background from hadron decays, especially from π^0 and η mesons. A criterion called the "isolation criteria", based on applying a threshold on the contributions of p_{T} from particles inside a cone around the photon candidate, is used to suppress the decay and fragmentation photons. This has led to the prescription of "isolated photons" as reported in Ref. [1], which is the first isolated photon measurement from ALICE.

The study of the dijet invariant mass also helps to probe the initial state, including cold nuclear matter effects or possible medium modifications in small collision systems. In heavy-ion collisions, it is an important tool to inspect the nuclear modification effects as dijets should have less surface bias than single jet measurements. These measurements in small systems provide an essential baseline for such studies in heavy-ion collisions.

2. Analysis details

Photons have been reconstructed using the Electromagnetic Calorimeter (EMCal) [2, 3] and the Di-jet Calorimeter (DCal) [4]. Charged-particle tracks have been obtained using the combination of the Inner Tracking System (ITS) [5] and the Time Projection Chamber (TPC) [6], which are part of the ALICE central tracking system (CTS). The Minimum Bias (MB) interaction trigger for both pp and pA collisions is based on the response of the V0 detector, consisting of two arrays of 32 plastic scintillators, located at $2.8 < \eta < 5.1$ (V0A) and $-3.7 < \eta < -1.7$ (V0C) [7].

The EMCal is a lead-scintillator sampling electromagnetic calorimeter used to measure the energy of photons, electrons, and the neutral part of jets via the electromagnetic showers produced inside it. It has a cellular structure made up of cells with a granularity of $\Delta\eta \times \Delta\varphi = 0.0143 \times 0.0143$ rad. The geometrical acceptance of the EMCal is $|\eta| < 0.7$ and $80^\circ < \varphi < 187^\circ$. The DCal is an extension of the EMCal. It is back-to-back in azimuth with respect to the EMCal and uses the same technology and material as the EMCal. It covers $0.22 < |\eta| < 0.7$ and $260^\circ < \varphi < 320^\circ$, and an additional region between $|\eta| < 0.7$ and $320^\circ < \varphi < 327^\circ$. It was installed and commissioned during the first long shutdown of the LHC and therefore was not operational during the data taking with pp collisions at $\sqrt{s} = 8$ TeV.

Thus, both the EMCal and the DCal are used in the trigger and analysis of the *pp* collisions at $\sqrt{s} = 13$ TeV and the *p*–Pb collisions at $\sqrt{s_{NN}} = 5.02$ TeV, while only the EMCal was used in the *pp* collisions at $\sqrt{s} = 8$ TeV. The analysed data were selected by the EMCal/DCal triggers at two levels: Level-0 (L0) and Level-1 (L1), in addition to the MB trigger condition [3].

The ITS consists of 6-layers of silicon detectors that surround the interaction point, spanning the full azimuth ($\Delta\varphi = 360°$) and $|\eta| < 0.9$. The two innermost layers consist of the Silicon Pixel Detectors (SPD) and are surrounded by the two layers of the Silicon Drift Detectors (SDD) followed by those of the two Silicon Strip Detectors (SSD). The TPC is a large (≈ 85 m^3) cylindrical drift detector covering $|\eta| < 0.9$ over the full azimuthal angle, with a maximum of 159 reconstructed space points along the track path. It was filled with a Ne/CO_2 gas mixture during the data taking with *pp* collisions at $\sqrt{s} = 8$ TeV, whereas a mixture of Ar/CO_2 was used during data taking with the other systems of concern. The TPC and ITS tracking points are matched to form the tracks and determine the momentum.

2.1. Isolated photons

In the calorimeters, particles are reconstructed via clusters. Clusters are formed when particles deposit their energy in several calorimeter cells. Clusters are selected by grouping all cells with common sides whose energy is above 100 MeV, starting from a seed cell with at least 500 MeV. The photon reconstruction method closely follows the one described in Ref. [1]. Since photons are neutral particles, first a veto is applied to reject the clusters from the hadronic or electron origin. Then to reject the elongated clusters from neutral meson decays, a selection has been applied based on the shape of the electromagnetic shower in the calorimeter using a cut of $0.1 < \sigma^2_{\rm long} < 0.3$, where $\sigma^2_{\rm long}$ is a parameter that takes into account the cluster elongation [1]. Finally, the isolation criterion has been applied to reduce the contamination from the fragmentation and decay photons. Such an isolation criterion has been constructed by defining a cone centered around the photon direction in the η–φ plane with a fixed radius, $R = \sqrt{(\eta_i - \eta_\gamma)^2 + (\varphi_i - \varphi_\gamma)^2} = 0.4$, and summing the transverse energy of other particles inside the cone ($p_{\rm T}^{\rm iso}$). The Underlying Event (UE) has been estimated using the charged-particle $p_{\rm T}$ contributions in cones which lie perpendicular to the selected clusters and has been subtracted from the $p_{\rm T}^{\rm iso}$ value in the isolation cone. In this work, a threshold of $p_{\rm T}^{\rm iso} < 1.5$ GeV/c with charged-particles only isolation has been set to extract the isolated-photon candidates. For *pp* collisions at $\sqrt{s} = 8$ TeV and *p*–Pb collisions at $\sqrt{s_{NN}} = 5.02$ TeV, the UE subtraction has been done whereas that for *pp* collisions at $\sqrt{s} = 13$ TeV, the UE subtraction is yet to be done.

2.2. Dijet invariant mass

For the reconstruction of the dijet invariant mass, only charged particles have been used as the full azimuthal acceptance is pivotal for the analysis. Tracks with $|\eta| < 0.9$ and $p_{\mathrm{T}} > 0.15$ GeV/c have been selected. Jets have been reconstructed using the anti-k_{T} algorithm with $p_{\mathrm{T}} > 10$ GeV/c, and a jet resolution parameter $R = 0.4$. The background has been estimated by the FASTJET package [8], where k_{T} jets have been used without any kinematical cut. The background is subtracted both for pp and p–Pb systems as outlined in Refs. [9] and [10]. The invariant mass of the two jets depends on the transverse momentum and the geometry of the two jets. It is defined as, $M_{jj}^2 = (p_1 + p_2)^2 \approx 2p_{\mathrm{T},1}p_{\mathrm{T},2}(\cosh(\eta_1 - \eta_2) - \cosh(\varphi_1 - \varphi_2))$, where 1 and 2 represent the two jets forming the dijet, using the approximation for low mass jets. The leading and the subleading jets are required to have $p_{\mathrm{T}} > 20$ GeV/c, in addition, the azimuthal angle between them is required to be more than $\pi/2$. An unfolding procedure has been applied to correct for the detector effects and the background fluctuations.

3. Results and discussions

The isolated photon cross sections as measured with the ALICE detector in pp collisions at $\sqrt{s} = 8$ and 13 TeV and in p–Pb collisions at $\sqrt{s_{NN}} = 5.02$ TeV are shown in Fig. 1. The published data of isolated photon cross section in pp collisions at $\sqrt{s} = 7$ TeV [1] can also be seen in the figure. The statistical errors are plotted with error bars and the systematic errors with open boxes. The systematic errors were evaluated by looking into the sensitivity of the cross section to the choice of the analysis cuts. The

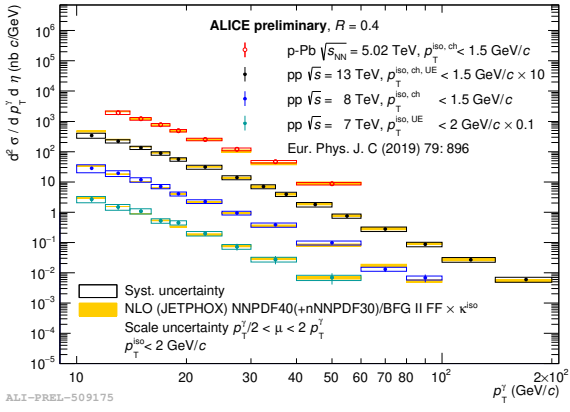

Fig. 1. (Colour online) Isolated photon cross section in pp collisions at $\sqrt{s} = 7$, 8, 13 TeV and in p–Pb collisions at $\sqrt{s_N} = 5.02$ TeV, compared with JETPHOX NLO calculations.

data have been compared to NLO calculations using JETPHOX [11] with NNPDF40 [12] and BFG II fragmentation function. The NLO scale uncertainty is shown with grey/yellow bands. The ALICE results extend the LHC measurements towards the lower p_{T} which will, in turn, aid measurements in lower x_{T} domain, since $x \approx x_{\mathrm{T}} = 2p_{\mathrm{T}}/\sqrt{s}$.

The isolated photon cross-section ratios in pp collisions at different energies along with the corresponding ratios calculated using NLO JETPHOX model have been calculated as can be seen in Fig. 2. The data and the NLO calculations are found to be consistent within uncertainties for the three different cases as mentioned below.

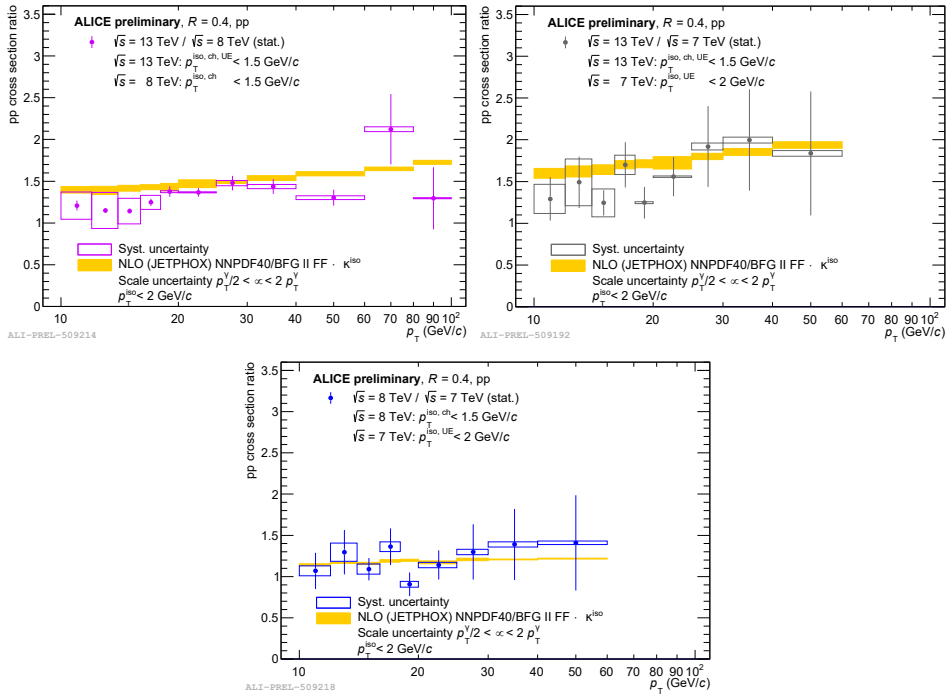

Fig. 2. Isolated photon cross section ratios in pp collisions: $\sqrt{s} = 13$ TeV/$\sqrt{s} = 8$ TeV (top left), $\sqrt{s} = 13$ TeV/$\sqrt{s} = 7$ TeV (top right), $\sqrt{s} = 8$ TeV/$\sqrt{s} = 7$ TeV (bottom).

The dijet invariant mass distribution has been measured in pp and p–Pb collisions at $\sqrt{s_{NN}} = 5.02$ TeV as shown in Fig. 3 along with the nuclear modification factor R_{pA}. This is the first dijet invariant mass measurement from ALICE and the value of R_{pA} is found to be unity within uncertainties. These results, among many others, can be used to quantify the medium induced modification of PDFs and fragmentation functions in Pb–Pb collisions in ALICE.

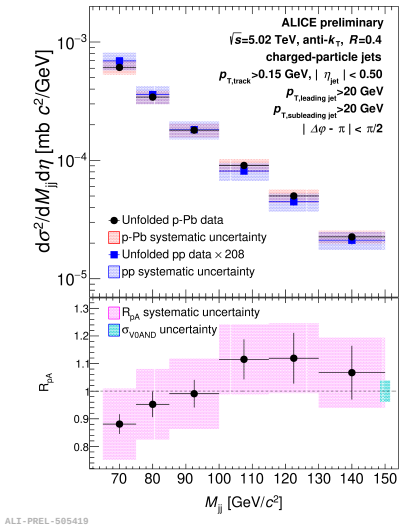

Fig. 3. Dijet invariant mass distribution in pp and p–Pb collisions at $\sqrt{s_{NN}} = 5.02$ TeV (top) and the nuclear modification factor R_{pA} (bottom).

REFERENCES

[1] ALICE Collaboration (S. Acharya *et al.*), *Eur. Phys. J. C* **79**, 896 (2019).

[2] ALICE Collaboration (P. Cortese *et al.*), CERN-LHCC-2008-014, CERN-ALICE-TDR-014.

[3] ALICE EMCal Collaboration (U. Abeysekara *et al.*), arXiv:1008.0413 [physics.ins-det].

[4] ALICE Collaboration (J. Allenet *et al.*), https://cds.cern.ch/record/1272952

[5] ALICE Collaboration (K. Aamodt *et al.*), *J. Instrum.* **5**, P03003 (2010), arXiv:1001.0502 [physics.ins-det].

[6] J. Alme *et al.*, *Nucl. Instrum. Methods Phys. Res. A* **622**, 316 (2010), arXiv:1001.1950 [physics.ins-det].

[7] ALICE Collaboration (E. Abbas *et al.*), *J. Instrum.* **8**, P10016 (2013), arXiv:1306.3130 [nucl-ex].

[8] M. Cacciari, G.P. Salam, G. Soyez, *Eur. Phys. J. C* **72**, 1896 (2012).

[9] CMS Collaboration (S. Chatrchyan *et al.*), *J. High Energy Phys.* **1208**, 130 (2012).

[10] G. Soyez *et al.*, *Phys. Rev. Lett.* **110**, 162001 (2013).

[11] S. Catani *et al.*, *J. High Energy Phys.* **0205**, 028 (2002); P. Aurenche *et al.*, *Phys. Rev. D* **73**, 094007 (2006).

[12] NNPDF Collaboration (R.D. Ball *et al.*), *Eur. Phys. J. C* **82**, 428 (2022), arXiv:2109.02653 [hep-ph].